

*Letter to the Editor***A Statistical Analysis of  $\Delta$ PA for EGRET-Detected AGNs****X.Y. Hong, D.R. Jiang, and Z.Q. Shen**

Shanghai Astronomical Observatory, Chinese Academy of Sciences, 80 Nandan Road, Shanghai 200030, P.R. China

Received 3 July 1997 / Accepted 13 November 1997

**Abstract.** A statistical analysis of position angle differences ( $\Delta$ PA) between small- and large-scale structures of EGRET-detected AGNs has been made. The results show that  $\gamma$ -ray quasars have the alignment of radio jets, while  $\gamma$ -ray BL Lac objects have large  $\Delta$ PA. This may contribute to a better understanding of different blazar types and of the AGN unification scheme.

**Key words:** radio continuum: EGRET-detected AGNs – galaxies: radio jets

**1. Introduction**

Since the launch of the *Compton Gamma Ray Observatory*, the Energetic Gamma Ray Experiment Telescope (EGRET) has so far detected 42 AGNs with high-confidence identifications (Thompson et al. 1995; 1996; Mattox et al. 1997). All these AGNs belong to the blazar category. At high energy  $\gamma$ -ray band ( $\geq 300$  MeV), the EGRET-detected blazars show a very high spectral luminosity and short time variability (Montigny et al. 1995). The  $\gamma$ -ray flare is often accompanied by a flare at low frequencies (e.g. Reich et al. 1993; Pohl et al. 1995; Lichti et al. 1995). All this evidence indicates that the  $\gamma$ -ray emission from the flaring blazars most probably is beaming nonthermal radiation supporting the relativistic beaming hypothesis and the unified scheme for AGNs (Schlickeiser 1996). The high energetic emission has been explained with the non-thermal Synchrotron Self Compton models or inverse Compton scattering of external soft photon (Melia & Konigl 1989; Dermer & Schlickeiser 1992; 1993; Bloom & Marscher 1993; Maraschi et al. 1993; Sikora et al. 1994; Ghisellini et al. 1996).

The fact that all EGRET-detected blazars are radio loud indicates that there is a strong relation between  $\gamma$ -ray and radio emission. Radio loud AGNs usually show core-jet structures (Pearson & Readhead 1988). It is generally believed that the

energy of the large scale structure is supplied by the central object through the small scale jet (Blandford & Rees 1974; Scheuer 1974). The jet directions are not always aligned from pc- to kpc-scale. The distribution of the apparent misalignment between the position angles of pc- and kpc-scale jets in core dominated radio sources shows an unexpected bimodal form with one peak close to  $0^\circ$  and the other near  $90^\circ$  (Pearson & Readhead 1988; Wehrle et al. 1992; Conway & Murphy 1993; and Xu et al. 1994).

In this paper we investigate the  $\Delta$ PA distribution of EGRET-detected sources, identified both with quasars and with BL Lac objects. In Sect. 2, we describe the collection of radio information in the EGRET-detected sample. In Sect. 3, we present statistical results of  $\Delta$ PAs of available  $\gamma$ -ray AGNs and discussion of those results.

**2. The sample**

The 42 EGRET-detected AGNs with high-confidence are listed in Table 1. Available position angles of radio jets of the EGRET-detected sources both at large- and small-scales are collected from the literature by using the NASA/IPAC Extragalactic Database. Blazars often show curve jet structures with multi-components in their radio images. In order to minimize a possible bias, we selected the PAs at jet components with comparable projective distances for all objects. Because the view angle information is unavailable (angle to the line of sight), the projective separation is used as a criterion to discriminate pc- or kpc-scale jets. The position angles are obtained from VLBI results at average projective distance of 10 pc and VLA or MERLIN observations at average projective distance of 17 kpc for two different scales respectively.

The projective distance can be calculated using the angular distance  $D_a = D_L/(1+z)^2$  to the object, where

$$D_L = \frac{c}{q_0^2 H_0} \left( z q_0 + [q_0 - 1] \left[ \sqrt{1 + 2z q_0} - 1 \right] \right), \quad (1)$$

where  $c$  is the speed of light,  $z$  is the redshift,  $H_0$  is the Hubble constant, and  $q_0$  is the deceleration parameter (Weinberg 1972). The values  $H_0=100$  km s $^{-1}$  Mpc $^{-1}$  and  $q_0=0.5$  are used in this paper.

**Table 1.** The position angle information of 42  $\gamma$ -ray AGN

source (1)	ID (2)	z (3)	$PA_{kpc}$ (4)	$r_{kpc}$ (5)	$ref_{kpc}$ (6)	$PA_{pc}$ (7)	$r_{pc}$ (8)	$ref_{pc}$ (9)	$\Delta PA$ (10)	ref (11)	Note (12)
0202 + 149	Q	0.833	unr.		MU93	292		BO96			1
0208 - 512	Q	1.003				233	8.3	TI96			
0234 + 285	Q	1.213	-25	30.1	MU93	-10	4.3	FE96	15		
0235 + 164	B	0.940	-37	16.9	MU93	45		MU90	82		2
0336 - 019	Q	0.852	-15	21.6	PE82	9	12.0	WE92	24	AP96	3
0420 - 014	Q	0.915	180	33.7	AN85	-147	4.6	FE96	33		
0440 - 003	Q	0.850	e-w	10.4	PE82	102	11.3	FE97	12		4
0446 + 112	Q	1.207	270	10.8	PE82						
0458 - 020	Q	2.286	-126	7.9	BR89	-55	15.8	WE92	71	AP96	
0521 - 365	Q	0.054	305	4.3	KE86	310	5.6	TI96	5		
0528 + 134	Q	2.060	0	8.1	PE82	24	4.4	PO95	24		
0537 - 441	B	0.896	305	30.2	PE82	5	16.8	TI96	60		
0716 + 714	B	0.30	-60	20.6	PE82	16	5.5	WI86	76		
0735 + 178	B	0.424	170	6.0	PE82	60	13.9	GA89	110	MU90	
0827 + 243	Q	0.939	200	33.4	PE82						
0829 + 046	B	0.180	180	29.4	AN85						
0836 + 710	Q	2.172	200	5.2	PE82	214	7.2	PE88	14	PE88	
0954 + 556	Q	0.909	300	13.4	MU93						
0954 + 658	B	0.368	205	11.7	PE82	-65	9.2	MU90	90		
1101 + 384	B	0.031	83	17.1	AN85	-52	18.0	XU95	135	MU90	5
1127 - 145	Q	1.187	41	129	RU88	65	12.9	WE92	24	WE92	6
1156 + 295	Q	0.729	340	7.7	PE82	-5	10.0	FE96	15		
1219 + 285	B	0.102	250	16.3	AP96	110	7.5	AP96	140	AP96	
1222 + 216	Q	0.435				-15	11.5	HO92b	23	HO92a	7
1226 + 023	Q	0.158	222	37.3	PE82	-130	9.2	WA90	8		
1253 - 055	Q	0.538	202	17.2	PE82	-137	11.0	UN86	21	MU90	
1406 - 076	Q	1.494									
1424 - 418	Q	1.552	-10		PR89						8
1510 - 089	Q	0.361	160	24.4	PE82	173	12.2	RO84	13		
1606 + 106	Q	1.226	-90	25.8	MU93						
1611 + 343	Q	1.401	-170	21.5	MU93	-178	6.4	FE96	8		
1622 - 253	Q	0.786	303	8.2	PE82	6	7.4	FE96	63		
1633 + 382	Q	1.814	-60	0.8	XU95	-64	4.6	PE88	4		9
1730 - 130	Q	0.902	unr.			0	21.0	BO96			1, 10
1739 + 522	Q	1.375	260	15.0	PE82	319	8.6	AP96	59	AP96	
1830 - 210	Q	1.0									
1908 - 201											
2052 - 474	Q	1.489									
2200 + 420	B	0.086	unr.		UL83	183	3.2	PE88			1
2209 + 236	Q										
2230 + 114	Q	1.037	140	6.8	PE82	137	42.2	BA86	3	MU90	
2251 + 158	Q	0.859	-49	21.7	BR82	-65	41.7	PA84	16	BR86	

**Notes:** 1. The source was unresolved by VLA. 2. The position angle of VLBI jet component varied within  $10^\circ$  to  $45^\circ$  (MU90), the largest  $\Delta PA$  was chosen. 3. The  $\Delta PA=76^\circ$  or  $24^\circ$ ,  $24^\circ$  was selected here. 4. VLA result showed 3 components in east-west direction. 5. The PA of VLBI jet at 0.6 pc is  $-24^\circ$ . 6. A VLA image made at 1375 MHz (RU88) shows a weak, thin jet extending 30 arcseconds at  $PA=41^\circ$ . 7. The VLBI jet closely aligned with the MERLIN jet (HO92b). 8. Because of the low declination of the source 1424-418, no enough observed results to be deduced a  $\Delta PA$  at a comparable scale. 9. MERLIN image was used for  $PA_{kpc}$ . A jet at separation of 4 mas in  $PA -65^\circ$  curved to west. MERLIN image shows the elongation at  $PA=-40^\circ$ . VLA show a jet component at 3 arcseconds in  $PA=176^\circ$  curved to east. 10. VLA result of 1730-130 showed an unresolved core and a secondary component at  $PA = 273^\circ$  separated 11 arcsecond from the core. It is believed that the secondary has no connection to 1730-130 (RO84). This may indicate that the secondary component is not a jet component of 1730-130.

The sample is shown in Table 1. Column 1 lists the source name. Column 2 is the class (Q: quasar, B: radio selected BL Lac Object). Column 3 is redshift. Columns 4, 5, and 6 list the information of kpc jet, they are position angle, projective distance to the core in kpc, and the reference respectively. Columns 7, 8, and 9 list the position angle, projective distance to the core in pc, and reference of pc (VLBI) jet respectively. Column 10 is the  $\Delta PA$ . Column 11 is the reference of column 10. Some notes are listed in column 12.

In the sample, 6 sources have no kpc scale images in literature; 3 sources are unresolved by VLA; 11 sources lack VLBI images. As a result, the position angle differences are available for 27 EGRET-detected blazars, which are listed in Table 1.

### 3. Results and discussion

The distributions of the  $\Delta PA$  for 27 EGRET-detected blazars are shown in Fig. 1 (for quasars) and Fig. 2 (for BL Lac objects). The results reveal that  $\gamma$ -ray quasars have the alignment of radio jets (Fig. 1), while  $\gamma$ -ray BL Lac objects have large  $\Delta PA$  (Fig. 2). The average  $\Delta PA$  of quasars  $\overline{\Delta PA}_Q$  is  $21^\circ \pm 19^\circ$  and the average  $\Delta PA$  of BL Lac objects  $\overline{\Delta PA}_B$  is  $99^\circ \pm 30^\circ$ . The difference between the  $\overline{\Delta PA}_B$  and the  $\overline{\Delta PA}_Q$  is about  $3\sigma$ . It seems that the difference of two  $\Delta PA$  distributions is significant.

With some available core-dominated samples (e.g. Pearson & Readhead 1988, Wehrle et al. 1992), we can inspect the  $\Delta PA$  of  $\gamma$ -ray quiet blazars. Some well known superluminal quasars show disalignment in the radio jets (e.g. 3C345, 0906+430, 1458+718), while some superluminal BL Lac objects show alignment (e.g. 1308+326, 2007+777). We also note some alignment superluminal sources are not detected by EGRET (e.g. 3C120).

A  $\Delta PA$  which derived from radio observation may indicate a real bending of the radio jet or the result of projection of the jet trajectory onto the plane of the sky. In the later case, the projective  $\Delta PA$  can be written as a function of the inclination angles  $\theta$  and  $\theta'$  of the pc- and kpc-scale jet axes with respect to the line of sight and the real bending angle  $\Delta\phi$ ,

$$\cos(\Delta PA) = (\cos \Delta\phi - \cos \theta \cos \theta') / (\sin \theta \sin \theta'). \quad (2)$$

The Eq. (2) can be rewritten as,

$$\sin^2 \frac{\Delta PA}{2} = \frac{2 \sin^2(\Delta\phi/2) - 1 + \cos(\theta - \theta')}{2 \sin \theta \sin \theta'}, \quad (3)$$

which indicates  $\sin(\Delta PA/2)$  is inversely proportional to  $\theta$  ( $\sin(\Delta PA/2) \sim \Delta\phi/2\theta$ ) for small  $\theta$ ,  $\theta'$ , and  $\Delta\phi$  ( $\theta \approx \theta'$ ). It is clear that in the case of a closer alignment of the jet axis with the line of sight the observed misalignment between small- and large-scale jets is much more sensitive to a small deviation of the jet trajectory.

It is difficult to explain the observed jet misalignment of the jets in BL Lac objects with stronger external forces to the jets because of the absence or weakness of a broad line region in the BL Lac objects. The detection of BL Lac objects at TeV photon energies, together with the fact that the total energy output is

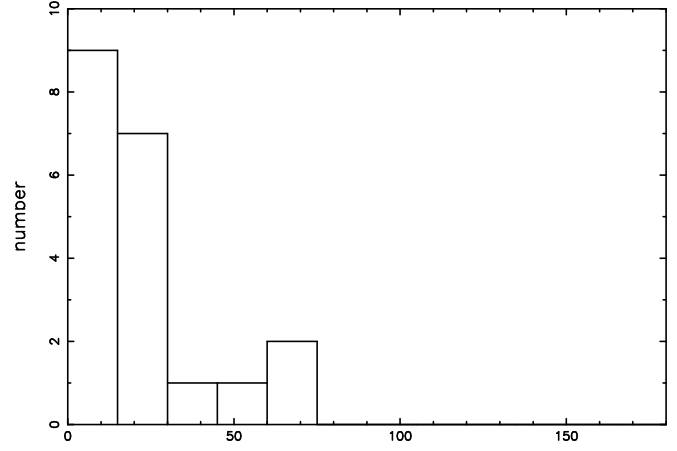


Fig. 1. The  $\Delta PA$  ( $^\circ$ ) distribution of EGRET-detected quasars

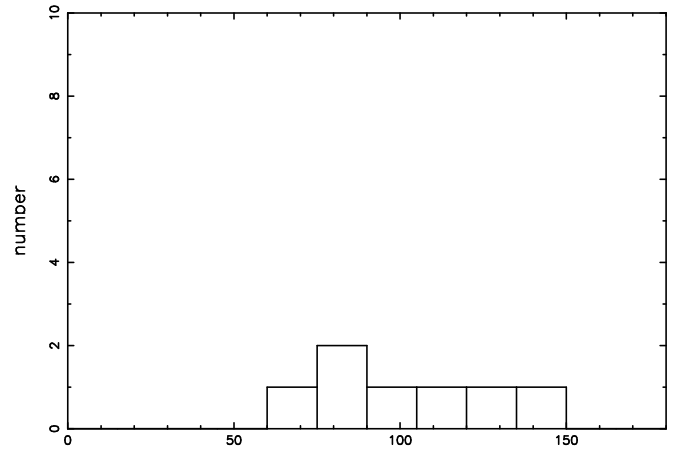


Fig. 2. The  $\Delta PA$  ( $^\circ$ ) distribution of EGRET-detected BL Lacs

dominated by radiation in the GeV to TeV regime, seems to indicate that the radiation emerging from the BL Lac objects is even more strongly Doppler boosted than in quasars. Obviously the large misalignment angles observed in BL Lac objects jets do not correspond to the real bending of the jets, but are the results of the projection of the jet trajectories onto the plane of the sky. Thus, the large misalignment angles in BL Lac objects indicate most probably a closer alignment of the jet structures with the line of sight in these objects. The radio jets of EGRET-detected BL Lac objects may be closer to the line of sight than that of  $\gamma$ -ray quiet sources, so the projective effect is much more obvious. The result is in agreement with the AGN unification schemes.

The VLBI polarization images revealed that the direction of the magnetic field tends to be parallel to the VLBI structure axis in quasars, while it tends to be perpendicular to the jet axis in BL Lac objects (Cawthorne et al. 1993). This may indicate that the  $\gamma$ -ray emission is related to the magnetic field.

It is also possible that the different  $\Delta PA$  distribution between EGRET-detected quasars and EGRET-detected BL Lac objects may be related to the properties of central objects. We are still not clear if the detection of  $\gamma$ -ray emission is dependent upon

the magnetic field in the jet, opaque medium surrounding the central engine, and so on. VLBI polarization observations are strongly encouraged to find the relationship.

In conclusion, the results presented in this paper may well contribute to a better understanding of different blazar types and the AGN unification scheme. Much more radio observations are expected to be done to get the sample as complete as possible for further study.

*Acknowledgements.* This work is supported by Chinese Natural Science Foundation. The authors are very grateful to the referee Dr. M. Böttcher for his valuable comments and corrections. The research has made extensive use of the NASA/IPAC Extragalactic Database (NED), which is operated by the Jet Propulsion Laboratory, California Institute of Technology.

## References

- Antonucci R. R. J. and Ulvestad J. S., 1985, ApJ 294, 158. AN85  
 Appl S., Sol H., and Vicente L., 1996, A&A 310, 419. AP96  
 Baath L. B., 1987, in: Superluminal Radio Sources, eds. J. A. Zensus and T. J. Pearson (Cambridge: Cambridge Univ. Press), p. 206. BA86  
 Blandford R. D. and Rees M. J., 1974, MNRAS 165, 395  
 Bloom S. D. and Marscher A. P., 1993, in Proceeding of the Compton Symp., eds. N. Gehrels and M. Friedlander, New York, AIP, p. 578  
 Bondi M., Padrielli L., Fanti R. et al., 1996, A&A 308, 415. BO96  
 Browne I. W. A., 1987, in: Superluminal Radio Sources, eds. J. A. Zensus and T. J. Pearson (Cambridge: Cambridge Univ. Press), p. 129. BR86  
 Browne I. W. A., Clark R. R., Moore P. K. et al., 1982, Nature 299, 788. BR82  
 Cawthorne T. V., Wardle J. F. C., Reborts D. H., and Gabuzda D. C., 1993, ApJ 416, 519  
 Conway J. E. and Murphy D. W., 1993, ApJ 411, 89  
 Dermer C. D. and Schlickeiser R., 1992, Sci 257, 1642  
 Dermer C. D. and Schlickeiser R., 1993, ApJ 416, 458  
 Fey A. L., Clegg A. W., and Fomalont E. B., 1996, ApJS 105, 299. FE96  
 Fey A. L. and Charlot P., 1997, ApJS 111, 95. FE97  
 Gabuzda D. C., Wardle J. F. C., Roberts D. H., 1989, ApJ 338, 743, GA89  
 Ghisellini G., Maraschi L. and Dondi L., 1996, A&AS, Special issue third Compton symposium, 120, 503  
 Hooimeyer J. R. A., Barthel P. D., Schilizzi R. T., and Miley G. K., 1992, A&A 261, 18. HO92a  
 Hooimeyer J. R. A., Schilizzi R. T., Miley G. K., and Barthel P. D., 1992, A&A 261, 25. HO92b  
 Keel W. C., 1986, ApJ 302, 296. KE86  
 Lichti G. G., et al., 1995, A&A 298, 711  
 Mattox J.R., Schachter J., Molnar L. et al., 1997, ApJ 481, 95  
 Maraschi L., Ghisellini G., and Celotti A., 1993, ApJ 397, L5  
 Melia F. & Konigl A., 1989, ApJ 340, 162  
 Montigny von C., Bertsch D. L., Chiang J. et al., 1995, ApJ 440, 525  
 Murphy D. W., Browne I. W. A., and Perley R. A., MNRAS 1993, 264, 298. MU93  
 Mutel R. L., 1990, in: Parsec-scale Radio Jets, eds. J. A. Zensus and T. J. Pearson (Cambridge: Cambridge Univ. Press), p. 98. MU90  
 Pauliny-Toth I. I. K., Porcas R. W., Zensus A. et al., in: IAU Symposium 110, VLBI and Compact Radio Sources, eds. R. Fanti, K. Kellermann, and S. Setti (Dordrecht: Reidel), p. 149. PA84  
 Perley R. A., 1982, AJ 87, 859. PE82  
 Pearson T. J. and Readhead A. C. S., 1988, ApJ 328, 114. PE88  
 Pohl M., Reich W., Krichbaum T. P. et al., 1995 A&A 303, 383. PO95  
 Preston R. A., Jauncey D. L., Meier D. L. et al., 1989, AJ 98, 1. PR89  
 Reich W., et al., 1993, A&A 273, 65  
 Romney J., Padrielli L., Barthel N. et al., 1984, A&A 135, 289. RO84  
 Rusk R. E., 1988, PhD. thesis, Univ. Toronto. RU88  
 Scheuer P. A. G., 1974, MNRAS 166, 513  
 Schlickeiser R., 1996, A&ASS 120, 481  
 Sikora M., Begelman M. C., and Rees M. J., 1994, ApJ 421, 153.  
 Thompson D. J., Bertsch D. L., Dingus B. L. et al., 1995, ApJS 101, 259  
 Thompson D. J., Bertsch D. L., Dingus B. L. et al., 1996, ApJS 107, 227  
 Tingay S. J., Edwards P. G., Costa M. E. et al., 1996, ApJ 464, 170. TI96  
 Ulvestad J. S., Johnston K. J., and Weiler K. W., 1983, ApJ 266, 18. UL83  
 Unwin S. C., 1987, in: Superluminal Radio Sources, eds. J. A. Zensus and T. J. Pearson (Cambridge: Cambridge Univ. Press), p. 34. UN86  
 Wardle J. F. C., Robert D. H., and Brown L. F. et al., in: Parsec-scale Radio Jets, eds. J. A. Zensus and T. J. Pearson (Cambridge: Cambridge Univ. Press), p. 20. WA90  
 Wehrle A. E., Cohen M. H., Unwin S. C. et al., 1992, ApJ 391, 589. WE92  
 Weinberg, S., Gravitation And Cosmology, 1972, John Wiley & sons, New York, Printed in United States America.  
 Witzel A., 1987, in: Superluminal Radio Sources, eds. J. A. Zensus and T. J. Pearson (Cambridge: Cambridge Univ. Press), p. 83. WI86  
 Xu W., Readhead A. C. S., and Pearson T. J. et al. 1994, in: Compact Extragalactic Radio Sources, eds. J.A. Zensus and K. I. Kellermann, p. 7  
 Xu W., Readhead A. C. S., and Pearson T. J. et al., 1995, ApJS 99, 297. XU95

This article was processed by the author using Springer-Verlag L<sup>A</sup>T<sub>E</sub>X A&A style file L-AA version 3.